



**HAL**  
open science

## Assessing functional and structural cardiotoxicity in cultured human iPSC-cardiomyocytes in a single plate format

Liang Guo, Mike Furniss, Levy Batista, Thierry Bastogne, Yan Zhuge, Joseph Wu, Sandy Eldridge, Myrtle Davis

### ► To cite this version:

Liang Guo, Mike Furniss, Levy Batista, Thierry Bastogne, Yan Zhuge, et al.. Assessing functional and structural cardiotoxicity in cultured human iPSC-cardiomyocytes in a single plate format. Safety Pharmacology Society 2017 Annual Meeting, SPS 2017, Sep 2017, Berlin, Germany. hal-01669498

**HAL Id: hal-01669498**

**<https://hal.science/hal-01669498v1>**

Submitted on 20 Dec 2017

**HAL** is a multi-disciplinary open access archive for the deposit and dissemination of scientific research documents, whether they are published or not. The documents may come from teaching and research institutions in France or abroad, or from public or private research centers.

L'archive ouverte pluridisciplinaire **HAL**, est destinée au dépôt et à la diffusion de documents scientifiques de niveau recherche, publiés ou non, émanant des établissements d'enseignement et de recherche français ou étrangers, des laboratoires publics ou privés.

# Assessing functional and structural cardiotoxicity in cultured human iPSC-cardiomyocytes in a single plate format

L. Guo, M. Furniss, J. Hamre, L. Batista\*, T. Bastogne\*, Y. Zhuge#, J.C. Wu#, S. Eldridge†, M. Davis†

Laboratory of Investigative Toxicology, Frederick National Laboratory for Cancer Research/Leidos Biomedical Research, Inc., Frederick, MD 21702; \*University of Lorraine, INRIA, Vandœuvre-lès-Nancy, France

#Stanford Cardiovascular Institute, Stanford University, Stanford, CA 94305

†DCTD, National Cancer Institute, Bethesda, MD 20892

## Abstract

A comprehensive profiling of cardiotoxicity early in drug discovery and development can aid in reducing late-stage attrition and establishing risk-mitigation strategies during clinical development. In most cases, multiple assay platforms and instrument-specified plate formats are required for this type of approach. In this study, we evaluated both functional and structural endpoints associated with cardiotoxicity in human induced pluripotent stem cell-derived cardiomyocytes (hiPSC-CMs) cultured in a single 384-well plate. We measured intracellular Ca<sup>2+</sup> transit, caspase 3/7 activation and plasma membrane permeabilization sequentially in the same plate via a series of assay readouts. A set of cardiac ion channel modulators (dofetilide, sotalol, nifedipine and mexiletine) and chemotherapeutics (tamoxifen, nilotinib, sunitinib and doxorubicin) was tested at clinically relevant concentrations for effects on intracellular Ca<sup>2+</sup> transits after a short-term (30 minutes) exposure, and plasma membrane permeabilization and caspase 3/7 activation after a long-term (72 hours) exposure. Intracellular Ca<sup>2+</sup> transits were monitored by fluorescent images taken with a high-speed camera in beating cardiomyocytes loaded with Cal520® Ca<sup>2+</sup> dye, permeabilized plasma membrane (for dead-cell detection) was identified with live-stain DRAQ7™ nuclear dye and activation of caspase 3/7 was determined biochemically with the Caspase-Glo® 3/7 Assay kit. Multiple endpoints derived from Ca<sup>2+</sup> transits, including beat rate, calcium transit duration (CTD) measured at 30% or 90% from peak and corrected by inter-peak interval (IPI), along with CTD triangulation, beat rhythm, short- or long-term variability of CTD90 and IPI Poincaré plots, were used to assess drug effects on intracellular Ca<sup>2+</sup> cycling and arrhythmogenicity. Increases in positive nuclear staining for DRAQ7™ and caspase 3/7 activity represented structural cardiotoxicity. We found that increased CTD triangulation, development of arrhythmic events and both the short- and long-term variability of CTD90 or IPI were robust indicators of functional effects. Positive nuclear staining for DRAQ7™ was a robust indicator of structural effects. Accordingly, dofetilide and sotalol were identified as primarily arrhythmogenic, doxorubicin was primarily structurally toxic, while nilotinib and sunitinib were both arrhythmogenic and structurally toxic. The use of these endpoints in a single plate format simplifies the cardiotoxicity assessment and does not require multiple cell plates for measurements.

## Results

### Ca<sup>2+</sup> transits of beating cardiomyocytes:

Figure 1. Ca<sup>2+</sup> cycling imaged at 51 fps from a single view-field

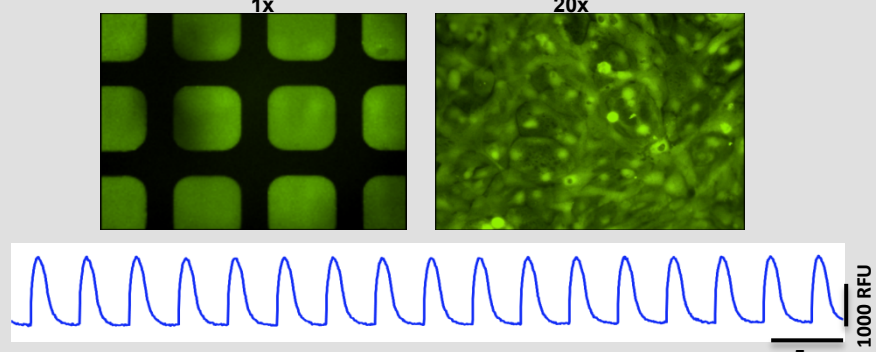
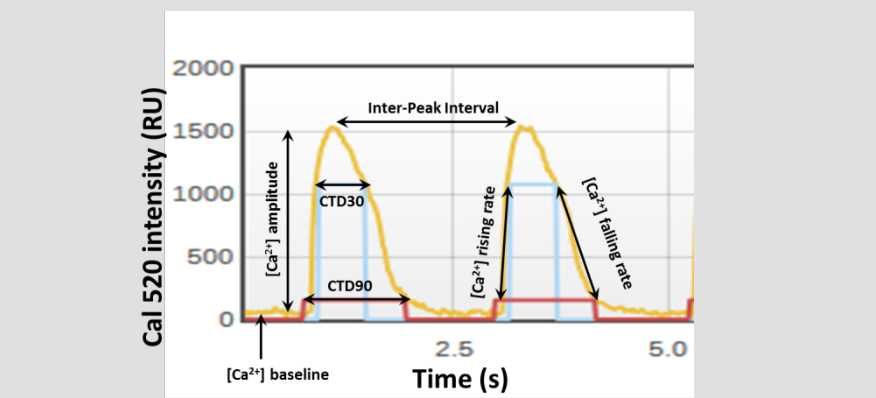


Figure 2. Ca<sup>2+</sup> transits analyzed by CYBERnano i-Cardio



Parameters: Beat rate, Inter-Peak Interval (IPI), [Ca<sup>2+</sup>] baseline, amplitude, rising rate (RR), falling rate (FR), transit duration 30 or 90 (CTD30 or CTD90), corrected CTD30 or 90 by IPI (CTDc = CTD(n)/IPI(n-1); Triangulation index: = CTD90/CTD30

Figure 3. Representative traces of typical effects on Ca<sup>2+</sup> transits

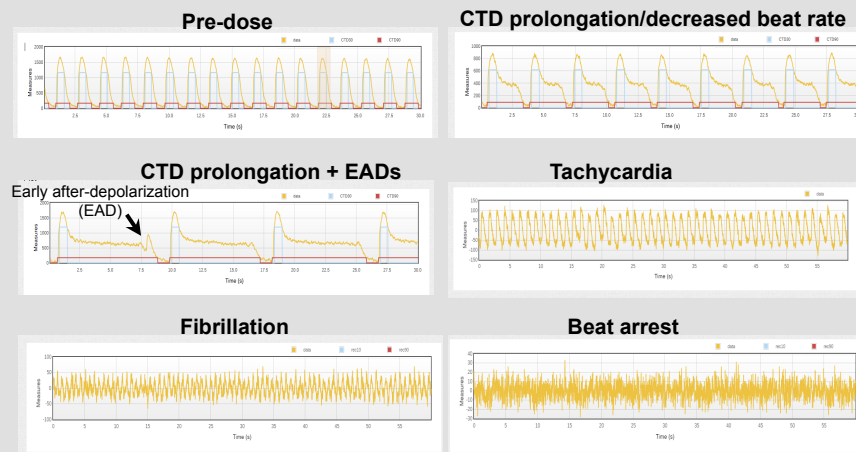


Table 1. Summary of effects on Ca<sup>2+</sup> transit parameters

| Drug ID               | Conc. (µM) | Beat rate | [Ca <sup>2+</sup> ] Baseline | [Ca <sup>2+</sup> ] Amplitude | Rising Rate | Falling Rate | CTD90     | CTD 30   | Corrected CTD90 | Corrected CTD30 | Triangulation Index |
|-----------------------|------------|-----------|------------------------------|-------------------------------|-------------|--------------|-----------|----------|-----------------|-----------------|---------------------|
| Vehicle               | 0.1% DMSO  | 106 ± 1   | 106 ± 2                      | 104 ± 5                       | 107 ± 5     | 113 ± 4      | 93 ± 2    | 94 ± 2   | 96 ± 1          | 95 ± 1          | 102 ± 1             |
| Dofetilide (0.006 µM) | 0.003      | 132# ± 9  | 98 ± 1                       | 68# ± 4                       | 82# ± 5     | 84# ± 9      | 88 ± 5    | 93 ± 11  | 115# ± 1        | 121# ± 8        | 95 ± 6              |
|                       | 0.01       | 155# ± 7  | 104 ± 4                      | 56# ± 6                       | 61# ± 19    | 63# ± 21     | 82# ± 1   | 71# ± 11 | 126# ± 5        | 108 ± 16        | 121# ± 12           |
|                       | 0.03       | 213# ± 3  | 96 ± 1                       | 27# ± 0                       | 22# ± 0     | 39# ± 2      | 54# ± 0   | 37# ± 1  | 114# ± 2        | 79# ± 1         | 145# ± 4            |
| Sotalol (14.7 µM)     | 0.1        | 104 ± 1   | 116 ± 1                      | 94 ± 2                        | 94 ± 3      | 101 ± 2      | 92 ± 2    | 89 ± 1   | 96 ± 1          | 93 ± 2          | 103 ± 3             |
|                       | 1          | 104 ± 2   | 112 ± 4                      | 90 ± 2                        | 90 ± 2      | 92 ± 5       | 95 ± 1    | 91 ± 1   | 99 ± 0          | 95 ± 1          | 104 ± 0             |
|                       | 10         | 100 ± 2   | 109 ± 2                      | 93 ± 4                        | 106 ± 9     | 94 ± 5       | 105# ± 2  | 112# ± 6 | 105 ± 2         | 111# ± 4        | 95 ± 3              |
| Nifedipine (0.19 µM)  | 0.001      | 99 ± 4    | 113 ± 3                      | 98 ± 1                        | 103 ± 9     | 101 ± 3      | 92 ± 2    | 88 ± 0   | 96 ± 3          | 92 ± 3          | 105 ± 2             |
|                       | 0.01       | 107 ± 3   | 111 ± 4                      | 112 ± 2                       | 115 ± 5     | 118 ± 4      | 93 ± 1    | 100 ± 2  | 100 ± 2         | 97 ± 3          | 103 ± 1             |
|                       | 0.1        | 76# ± 3   | 70# ± 1                      | 54# ± 3                       | 52# ± 8     | 57# ± 3      | 51# ± 1   | 42# ± 0  | 49# ± 2         | 48# ± 2         | 101 ± 1             |
| Mexiletine (11.2 µM)  | 0.1        | 103 ± 2   | 117 ± 3                      | 95 ± 2                        | 91 ± 4      | 91 ± 2       | 97 ± 3    | 91 ± 4   | 99 ± 4          | 93 ± 5          | 107 ± 2             |
|                       | 1          | 97 ± 1    | 118 ± 2                      | 103 ± 2                       | 104 ± 2     | 99 ± 1       | 98 ± 1    | 94 ± 2   | 94 ± 1          | 90 ± 1          | 104 ± 1             |
|                       | 10         | 96 ± 2    | 106 ± 2                      | 89# ± 5                       | 84# ± 3     | 87# ± 3      | 100 ± 1   | 97 ± 2   | 96 ± 3          | 94 ± 2          | 102 ± 2             |
| Tamoxifen (0.11 µM)   | 0.1        | 114 ± 1   | 95 ± 2                       | 89 ± 3                        | 82 ± 7      | 105 ± 5      | 85 ± 2    | 83 ± 4   | 97 ± 2          | 95 ± 2          | 103 ± 1             |
|                       | 0.3        | 110 ± 2   | 107 ± 5                      | 112 ± 10                      | 117 ± 11    | 126 ± 13     | 88 ± 2    | 88 ± 3   | 97 ± 2          | 96 ± 4          | 101 ± 2             |
|                       | 1          | 110 ± 2   | 94 ± 1                       | 96 ± 4                        | 93 ± 6      | 95 ± 7       | 86 ± 2    | 86 ± 3   | 95 ± 3          | 95 ± 5          | 101 ± 2             |
| Nilotinib (0.84 µM)   | 0.1        | 98 ± 1    | 99 ± 2                       | 83# ± 1                       | 85# ± 5     | 86# ± 11     | 107 ± 6   | 114# ± 6 | 104 ± 6         | 111# ± 7        | 94 ± 2              |
|                       | 3          | 83# ± 13  | 98 ± 3                       | 71# ± 7                       | 80# ± 9     | 49# ± 17     | 149# ± 35 | 118# ± 5 | 114# ± 4        | 97 ± 13         | 124# ± 10           |
|                       | 30         | 162# ± 7  | 92# ± 0                      | 27# ± 3                       | 14# ± 2     | 21# ± 2      | 73# ± 2   | 33# ± 2  | 115# ± 2        | 52# ± 2         | 234# ± 14           |
| Sunitinib (0.18 µM)   | 0.1        | 111 ± 2   | 110 ± 0                      | 96 ± 6                        | 108 ± 3     | 117 ± 9      | 85 ± 1    | 86 ± 2   | 95 ± 1          | 96 ± 1          | 99 ± 1              |
|                       | 0.3        | 104 ± 5   | 108 ± 2                      | 87# ± 3                       | 117 ± 11    | 100 ± 5      | 95 ± 2    | 105 ± 6  | 99 ± 6          | 110 ± 12        | 91 ± 4              |
|                       | 1          | 88# ± 3   | 110 ± 3                      | 75# ± 4                       | 87# ± 7     | 72# ± 4      | 107# ± 3  | 111# ± 3 | 94 ± 3          | 98 ± 4          | 96 ± 2              |
| Doxorubicin (6.7 µM)  | 0          | 116 ± 2   | 109 ± 2                      | 91 ± 2                        | 96 ± 4      | 102 ± 3      | 87 ± 2    | 84 ± 3   | 100 ± 2         | 96 ± 2          | 104 ± 1             |
|                       | 0.3        | 117 ± 5   | 112 ± 2                      | 100 ± 8                       | 110 ± 7     | 110 ± 9      | 87 ± 1    | 84 ± 1   | 102 ± 4         | 98 ± 5          | 104 ± 2             |
|                       | 1          | 115 ± 2   | 106 ± 3                      | 96 ± 3                        | 101 ± 7     | 104 ± 4      | 89 ± 2    | 86 ± 3   | 102 ± 3         | 99 ± 5          | 104 ± 2             |

(mean ± SEM, n = 3-6 wells/group; #, P < 0.05 compared to vehicle with t-test; ND, not determined)

## Introduction

Cardiotoxicity is frequently a dose-limiting toxicity associated with many highly efficacious chemotherapeutics that include both classic cytotoxic or cytostatic agents, such as doxorubicin or other anthracycline analogs, and newly developed targeted anti-cancer molecules such as protein kinase inhibitors (i.e. sunitinib, dasatinib and nilotinib). As this adverse effect can be manifested by either structural damage (i.e. cardiomyopathy and heart failure) or functional alteration (i.e. arrhythmia and sudden cardiac death), evaluation on risks to induce both structural and functional cardiotoxicity should be included in preclinical safety profiling of each new anti-cancer drug prior to the first dose in human.

Human induced pluripotent stem cell-derived cardiomyocytes (hiPSC-CMs) represent a novel cellular model system to test for cardiotoxicity and are being used increasingly with a wide variety of analytic platforms in study of cardiac biology and drug safety testing. In this study, we developed an image-based, multiplex assay that enables interrogation of both functional and structural toxicity endpoints in a single plate format.

## Methods & Materials

### Cells:

Cryopreserved iPSC-cardiomyocytes were provided by Dr. Joseph C. Wu and Stanford Cardiovascular Institute (SCVI) Biobank

### Reagents:

RPMI 1640, BD Matrigel (Fisher/Corning); B27-insulin, DMEM/F12 (Gibco/Life Science); Accutase (Sigma); Cal-520® Ca<sup>2+</sup> dye (AAT Bioquest), DRAQ7™ DNA dye (abcam), Caspase-Glo 3/7 assay kit (Promega); Dofetilide, sotalol, nifedipine, mexiletine, tamoxifen, nilotinib, sunitinib and doxorubicin (NCI Compound Repository)

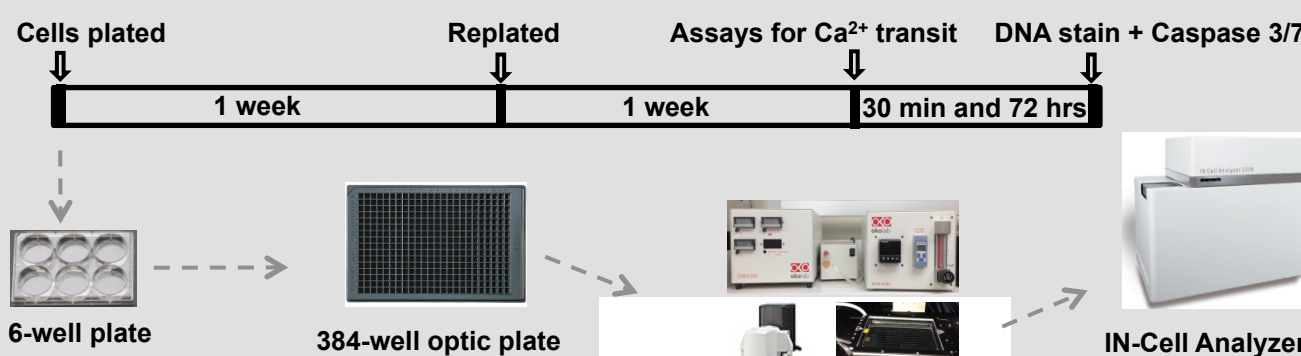
### Biomarkers:

Ca<sup>2+</sup> transits: contractile function, repolarization-delay, arrhythmia

DNA stain: permeabilization of plasma membrane (cell death)

Caspase 3/7 activity: apoptosis activation

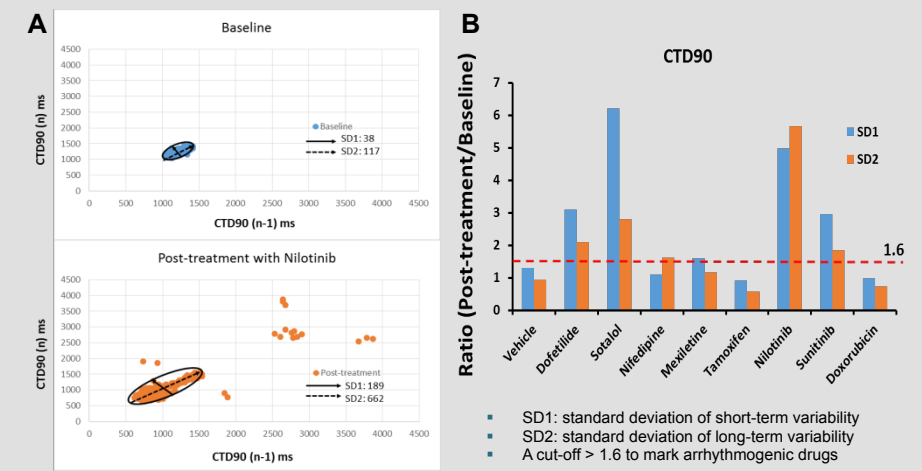
## Workflow:



### Data analysis:

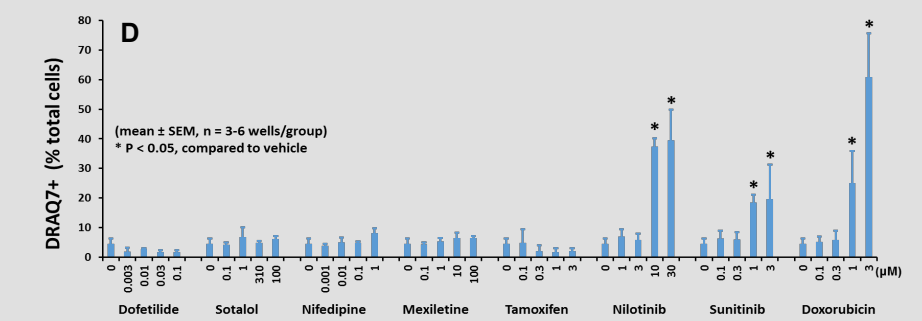
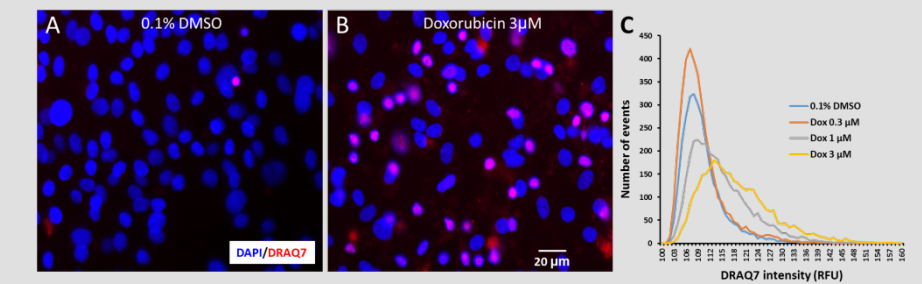
Measurement of beat-to-beat Ca<sup>2+</sup> transits was performed by CYBERnano i-Cardio platform; treatment-related changes in each endpoint were shown as % of the baseline value. Cells stained positive with DRAQ7 were shown as % of total nuclear (DAPI) counts and Caspase 3/7 activity was quantified as the luminescence intensity in each well. Statistic analysis was conducted with Student's t-test.

Figure 4. Beat variability analysis on Poincaré plots of CTD90



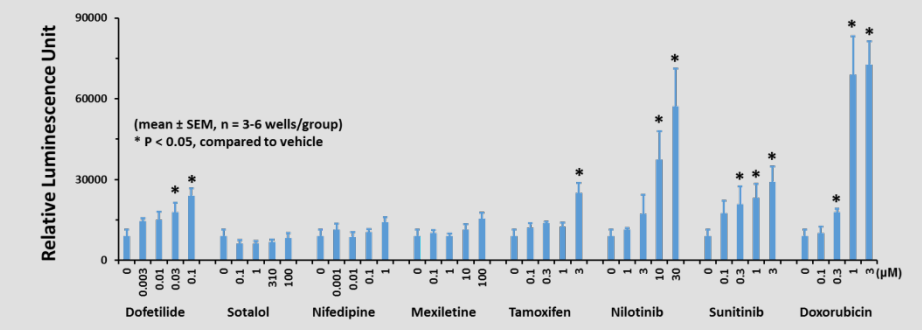
## Permeabilization of plasma membrane

Figure 5. Representative images of nuclear stains



## Activation of apoptosis

Figure 6. Caspase 3/7 activity



## Discussion & Conclusion

- Ca<sup>2+</sup> transits were sensitive to ion channel modulators, with changes in beat rate and Ca<sup>2+</sup> transit amplitude; EADs, beat-to-beat variability and triangulation of CTD were more specific than CTD lengthening to predict arrhythmogenesis
- Caspase 3/7 activity was a sensitive indicator of insults to hiPSC-CMs but increased nuclear stains of impermeable DNA dye was more robust to label structural cardiotoxicity

**Acknowledges:** The author thanks Drs. Ralph Parchment and Jerry Collins for managerial support. This project has been funded in whole or in part with federal funds from the National Institutes of Health, NHLBI HL117756 (JCW) and National Cancer Institute, under contract HHSN261200800001E. The content of this publication does not necessarily reflect the views or policies of the Department of Health and Human Services, nor does mention of trade names, commercial products, or organizations imply endorsement by the U.S. Government.